VILNIUS TECH
Vilnius Gediminas Technical University

Journal of Civil Engineering and Management
ISSN 1392-3730 / eISSN 1822-3605
2022 Volume 28 Issue 8: 601–619
https://doi.org/10.3846/jcem.2022.16995

VALORIZATION OF DIVERSE SIZES OF COAL BOTTOM ASH AS FINE AGGREGATE IN THE PERFORMANCE OF LIGHTWEIGHT FOAMED CONCRETE

Arian HADDADIAN[1,2], U. Johnson ALENGARAM[1*], Ahmed Mahmoud ALNAHHAL[1], Farhang SALARI[1], Karthick SRINIVAS M[1], Kim Hung MO[1], Sumiani YUSOFF[3], Muhammad Shazril Idris IBRAHIM[4]

[1]*Centre for Innovative Construction Technology (CICT), Department of Civil Engineering, Faculty of Engineering, Universiti Malaya, 50603 Kuala Lumpur, Malaysia*
[2]*ACE GREENCEMT Products Sdn. Bhd, Jalan Nilai 3/23, Bandar Baru Nilai, 71800 Nilai, Negeri Sembilan, Malaysia*
[3]*Institute of Ocean and Earth Sciences (IOES), Universiti Malaya, 50603 Kuala Lumpur, Malaysia*
[4]*Water Engineering and Spatial Environmental Governance (WESERGE), Department of Civil Engineering, Faculty of Engineering, Universiti Malaya, 50603 Kuala Lumpur, Malaysia*

Received 29 January 2022; accepted 25 April 2022

Abstract. In recent years, research work on the use of coal bottom ash (CBA) as a partial alternative for aggregate in concrete is on the rise. This research is aimed at examining the characteristics of lightweight foamed concrete with CBA as fine aggregate to produce environmentally sustainable product. With the volume replacement technique, CBA was used as 25%, 50%, 75%, and 100% replacement for conventional mining sand with different sieve sizes of smaller than 4.75, 2.36, and 0.6 mm in concrete. Water absorption, porosity as well as mechanical characteristics tests, including compressive strength, splitting tensile strength, and modulus of elasticity (MOE) were conducted and analyzed. X-ray diffraction and scanning electron microscopy microstructural investigations were also performed to correlate test results. The quality of concrete was investigated using a non-destructive ultrasonic pulse velocity test. According to the findings, the highest replacement level of CBA with a sieve size smaller than 0.6 mm had an impact in reducing workability. The effect of CBA particles on water absorption, MOE, compressive strength, and tensile strength depends on the size of the fine aggregate, the replacement ratio and the density. In general, substituting mining sand with CBA aggregate improved the mechanical performance of concrete, notably for the aggregate size of less than 0.6 mm. Moreover, the SEM images indicate that the addition of CBA particles decreased the size and quantity of voids in the foamed concrete.

Keywords: lightweight foamed concrete, compressive strength, splitting tensile strength, modulus of elasticity, microstructure, mining sand, coal bottom ash.

Introduction

Soil, energy, and water are among the most treasurable assets of humankind that contribute to climate change depending on their utilization method and extensiveness of exploration (Gielen et al., 2019). Extravagant exploitation of these worthy assets without regard for the natural environment would be detrimental to future generations. The United Nations General Assembly (UNGA) adopted Sustainable Development Goals (SDGs) in 2015 after realizing the grave consequences of inadequate resource management in the coming years. It established a framework for global collaboration in order to create a sustainable future (Gielen et al., 2019). At the same time, being one of the oldest industries, the construction sector continues to play an important role in human development and is responsible for contributing to this goal. The construction industry is the least sustainable in the world, using almost half of all non-renewable sources (Opoku, 2019). As a result, with the expected increase in the number of construction projects in the following years, there is a clear need to take a 'greener route' in the construction sector to

*Corresponding author. E-mail: *johnson@um.edu.my*

assure a more sustainable prospect (Bohari et al., 2017). Globally, the aggregate market is expected to grow at a pace of 5.2% each year (Gursel & Ostertag, 2019).

The demand for construction materials, particularly concrete, is now increasing as a result of the growing number of development projects. Concrete is the second most used material after water, and its production consumes a massive quantity of raw resources, leading to undesirable effects on the environment (Opon & Henry, 2019). As the need for concrete rises, more raw materials, such as fine and coarse aggregates, must be exploited from the environment. In Malaysia, sand and gravel production grew by nearly 11%, from more than 40 million tonnes in 2015 to nearly 45 million tonnes the following year (Muthusamy et al., 2020). One of the primary construction materials is natural sand. Excessive mining of natural sand from mines or mining would have a negative impact on the environment and living beings. Uncontrolled exploitation devastates the mining ecosystem, different aquatic species, and the local community's water sources (Sathiparan & De Zoysa, 2018). Other issues associated with sand mining include erosion, land loss, and an increase in poverty (Farahani & Bayazidi, 2018). The supply of natural sand has steadily declined during the last two decades. Another option is to crush the quarried stones into fine aggregate, but environmental and noise consequences make it unsuitable for green construction. Nevertheless, it would be more cost-effective and ecologically friendly to utilize industrial wastes instead of mining sand in concrete without altering the concrete's characteristics (Kassem et al., 2018). As a result, the current scarcity of raw materials underscores the importance of identifying alternative local waste materials generated constantly in massive amounts and may be used as fine aggregate replacements in mass concrete production.

Population growth and the associated demands for a more comfortable lifestyle have pushed up energy demand throughout time. Coal-fired power plants provide nearly 40% of the world's electricity (Muthusamy et al., 2020), making it critical to the iron and steel industry. According to current projections, coal-fired power plants are expected to provide almost half of the world's electricity in 2030 (Yao et al., 2015). Southeast Asia's energy demand has increased by 60% in the last 15 years (Mamat et al., 2019). Malaysia's energy supply increased from nearly 34,000 kilotonnes of oil equivalent (ktoe) in 1980 to more than 90,000 kilotonnes of oil equivalent (ktoe) in 2015, according to the Malaysia Energy Statistics Handbook 2017 (Malaysia Energy Commission, 2017). Future electricity generation is predicted to use less oil and more coal, with the latter accounting for up to 36.5% of total energy consumption (Chua & Oh, 2010). Malaysia Energy Statistics Handbook (Malaysia Energy Commission, 2017) states that coal is a natural resource utilized in electricity generation, with usage increasing from 8.3% in 1996 to more than 42% in 2015. Fly ash and bottom ash, the industry's waste products, have also risen in many parts of the world at the same period. In India, the US, Europe, and Malaysia together bottom ash production reaches millions of tonnes per year, causing environmental difficulties (Mangi et al., 2019).

Bottom ash from the combustion of coal is called coal bottom ash (CBA). Boilers produce this by-product, which accounts for 10–20% of coal ash (Argiz et al., 2018). According to its chemical composition, CBA is a complicated combination of metal carbonates and oxides (Tian et al., 2020). Because the ash is a waste product, it is dumped at a landfill or dumped in the water. Prior to being removed, bottom ash and fly ash are often combined in some power plants (Argiz et al., 2018). CBA discharge in the open air is dangerous to people and the environment (Singh & Siddique, 2016). Singh et al. (2018) reported the increased chance of skin, lung, and bladder cancer owing to CBA exposure. Additionally, due to the toxicity of ash disposal, it pollutes the environment, including the air and water supply. Besides, dumping slurry-type CBA in lakes can lead to a wide range of environmental issues (Shahbaz et al., 2016; Rathnayake et al., 2018). Indirectly, the management of CBA waste necessitates time, manpower, and financial resources. A major concern is the growing amount of ash being produced and the lack of suitable dumping sites. As a result, employing this material as one of the blended constituents in new concrete products will reduce the amount of landfill waste, as well as save time, money, and energy associated with removing it from the environment. With the use of this strategy, production costs would be reduced, and environmental protection would be improved by reducing waste (Siddique & Cachim, 2018).

In comparison with the natural aggregates, CBA possesses lower specific gravity because of the existence of voids in the particles (Singh & Siddique, 2016). Hence, the use of CBA as aggregate can decrease the density of the concrete (Baite et al., 2016). CBA can be classified as a pozzolanic material due to its high silica content (Kurama & Kaya, 2008; Singh et al., 2018). The properties of CBA particles have motivated researchers to examine the feasibility of using them as fine or coarse aggregates in concrete. Table 1 provides a summary of the experimental works performed on the impact of CBA on concrete's mechanical properties. In general, the compressive strength, flexural strength and modulus of elasticity of concrete comprising CBA is affected by the CBA replacement ratio, physical properties of CBA, and the w/c ratio (Singh et al., 2018).

It can be observed from the literature review those researchers aimed to examine the mechanical properties of the concrete comprising CBA. However, previous studies have paid attention to the possibility of using CBA as a fine aggregate in concrete production. On the other hand, the majority of earlier research focused on CBA as a 0 to 40% sand substitute. As a result, more research is required regarding using CBA as a sand replacement at a percentage of 50 to 100%. Besides, contradictory results can be found regarding the effects of using CBA on the

Table 1. Summary of past research on the use of CBA as aggregates in mortar and concrete

Reference	Country of research	CBA replacement ratio (%)	Effects		
			Compressive strength	Flexural strength	Young's modulus
Lee et al. (2010)	South Korea	0% to 30%	Reduced for all replacement ratios	Reduced for all replacement ratios	–
Onprom et al. (2015)	Thailand	0% to 30%	–	Enhanced at 10% replacement ratio	–
Kurama et al. (2009)	Turkey	25% to 100%	Reduced for all replacement ratios	–	–
Bai et al. (2005)	Northern Ireland	0% to 100%	Enhanced at 30% replacement ratio	–	–
Sachdeva and Khurana (2015)	India	20% to 50%	Reduced for all replacement ratios	Reduced for all replacement ratios	–
Yüksel and Genç (2007)	Turkey	10% to 50%	Reduced for all replacement ratios	Reduced for all replacement ratios	–
Yüksel et al. (2011)	Turkey	25% to 100%	Enhanced at 75% replacement ratio	–	–
Kurama and Kaya (2008)	Turkey	0% to 25%	Enhanced at 10% replacement ratio	Enhanced at 10% replacement ratio	–
Lee et al. (2010)	South Korea	0% to 100%	Enhanced at 25% replacement ratio	–	–
Kou and Poon (2009)	China	0% to 100%	Reduced for all replacement ratios	–	–
Topçu and Bilir (2010)	–	0% to 100%	Reduced for all replacement ratios	Reduced for all replacement ratios	Reduced for all replacement ratios
Sani et al. (2010)	Malaysia	10% to 50%	Reduced for all replacement ratios	–	–
Abubakar and Baharudin (2012)	Malaysia	10% to 50%	Reduced for all replacement ratios	–	–
Kim and Lee (2011)	Republic of Korea	25% to 100%	Reduced for all replacement ratios	Reduced for all replacement ratios	Reduced for all replacement ratios
Kumar et al. (2014)	India	0% to 20%	Enhanced at 10% replacement ratio	–	–
Siddique (2013)	India	0% to 30%	Reduced for all replacement ratios	–	–
Aswathy and Paul (2015)	India	10% to 50%	Enhanced at 20% replacement ratio	Enhanced at 30% replacement ratio	–
Singh and Siddique (2014)	India	0% to 100%	Reduced for all replacement ratios	–	Reduced for all replacement ratios
Hamzah et al. (2016)	Malaysia	5% to 30%	Enhanced at 10% replacement ratio	–	–
Kiran Kumar et al. (2018)	India	10% to 50%	Reduced for all replacement ratios	Reduced for all replacement ratios	Reduced for all replacement ratios
Muthusamy et al. (2018)	Malaysia	10% to 40%	Enhanced at 30% replacement ratio	–	–
Rafieizonooz et al. (2016)	Malaysia	0% to 100%	Enhanced at 50% replacement ratio	Enhanced at 50% replacement ratio	–
Balasubramaniam and Thirugnanam (2015)	India	10% to 30%	Enhanced at 10% replacement ratio	Enhanced at 10% replacement ratio	–
Bakoshi et al. (1998)	Japan	0% to 50%	Enhanced at 20% replacement ratio	Enhanced at 20% replacement ratio	–
Kasemchaisiri and Tangtermsirikul (2008)	Thailand	0% to 20%	Enhanced at 15% replacement ratio	–	–

mechanical properties of concrete. For instance, studies such as Sani et al. (2010), Topçu and Bilir (2010), Abubakar and Baharudin (2012), Siddique (2013), Kumar et al. (2014) concluded a negative response in compressive strength variation due to the replacement of fine aggregate with CBA. However, in some exceptional studies (Yüksel & Genç 2007; Singh & Siddique, 2014; Aswathy & Paul, 2015; Hamzah et al., 2016), the incorporation of CBA led to an enhancement in the compressive strength of concrete with varying degrees. Moreover, several studies have been performed on the replacement of CBA as natural aggregates in normal concrete. However, relatively limited research has been published on the use of CBA as fine aggregates replacement in lightweight foamed concrete (LFC), as one of the most well-known lightweight concretes (LWC). LFC is produced by mixing mortar and the foaming agent. There are various foaming agents, such as synthetic surfactants, carbon powder, hydrogen peroxide, Foaming C, SLS, stable foam, FoamTek, and aluminum powder (Singh & Siddique, 2016; Argiz et al., 2018; Tian et al., 2020). The presence of voids inside the LFC can highly reduce the weight and enhance the thermal insulation of concrete (Singh et al., 2018). LFC with higher water absorption capacity generally possesses lower compressive strength than normal concrete (Shahbaz et al., 2016). Generally, the strength of LFC is influenced by the water-to-cement ratio (w/c), air-to-cement ratio, sand-to-cement ratio (s/c), and properties of the foaming agent (Rathnayake et al., 2018). Foamed concrete is a well-known kind of lightweight concrete that is developed by combining mortar with foam. It offers a number of benefits over conventional OPC concrete, since the voids lower the density of concrete. In general, it is utilised to reduce noise and to enhance the insulating characteristics (Chung et al., 2019). The strength of foamed concrete is impacted not only by the water to cement ratio, but also by the air to cement ratio; the reduced air content caused by the high water to cement ratio, and the type of the foamed agent have an effect on the foamed concrete's strength (Falliano et al., 2018; Alnahhal et al., 2021, 2022). Additionally, the sand content of foamed concrete influences its compressive strength. It was reported that an increased sand to cement ratio decreased the strength of foamed concrete (Hamidah et al., 2005). Further, the use of FA in the lightweight concrete had been investigated (Majhi & Nayak, 2019; Patel et al., 2019; Satpathy et al., 2019; Majhi et al., 2021a, 2021b; Patel & Nayak, 2021). Researchers examined and reported the influence of CBA on the hardened characteristics of foamed concrete (Yang et al., 2019, 2020; Gencel et al., 2021).

Accordingly, this research aimed to examine the influence of CBA as fine aggregates replacement on the mechanical properties of LFC. First, the chemical and physical properties of CBA particles, including chemical compositions, specific gravity, and scanning electron microscope (SEM) images, were studied. Next, experimental studies were performed by replacing fine CBA with normal sand varying in replacement ratios (25%, 50%, 75%, and 100%). The investigated mechanical properties were workability, compressive strength, splitting tensile strength, water absorption, and modulus of elasticity.

1. Materials

1.1. Ordinary Portland cement (OPC)

The ordinary Portland cement (OPC) used in this study fulfilled the requirements of ASTM C150-14 (American Society for Testing and Materials [ASTM], 2014a). Table 2 shows the chemical composition, fineness, setting time, consistency, and compressive strength of the utilized cement.

Table 2. Chemical and physical properties of the utilized OPC and CBA

Chemical composition	FA (%)	CBA (%)	Physical properties (OPC)	
SiO_2	9.91	50.41	Fineness (m^2/kg)	281.4
Al_2O_3	2.76	15.52	Initial setting time (min)	125
Fe_2O_3	4.37	6.96	Final setting time (min)	210
CaO	64.00	2.53	Compressive strength (MPa)	
MgO	0.93	0.90	3 days	31.0
SO_3	2.30	0.32	7 days	38.9
K_2O	0.74	0.75	28 days	48.4
Na_2O	0.44	0.39	Consistency (%)	27
LOI	1.10	5.73	Specific gravity	3.15

1.2. Fine aggregates

A single source of CBA was collected from the Jimah power plant (Figure 1) located in Port Dickson, Malaysia. CBA was graded following the designation of ASTM C33/C33M-13 (ASTM, 2013a). CBA was sieved through a 4.75 mm sieve before being used to replace sand in this study. Figure 1 displays the scanning electron microscopic image of CBA particles which have irregular angular-shaped particles. The voids present on the particle surface indeed verifies the porous nature of the CBA, leading to higher water absorption of CBA particles than natural fine aggregates. Baite et al. (2016) reported the same results regarding the notable water absorption of CBA particles due to their porous nature. CBA was chemically analyzed and found to be mostly comprised of silica and alumina. CBA could be classified as Class-F pozzolan materials in accordance with ASTM C618-14 (ASTM, 2014b). The physical characteristics of CBA employed in this investigation are given in Table 3. Loss of ignition (LOI) was calculated using a muffle furnace according to ASTM C114-14 (ASTM, 2014c).

The mining sand was used as conventional fine aggregate. The fine aggregate complied with the requirements of ASTM C778-13 (ASTM, 2013b). Physical properties of the utilized mining sand are given in Table 3. The maximum size of the mining sand used in this research was 4.75 mm. Sieve analysis was conducted based on ASTM C136/C136M-14 (ASTM, 2014d).

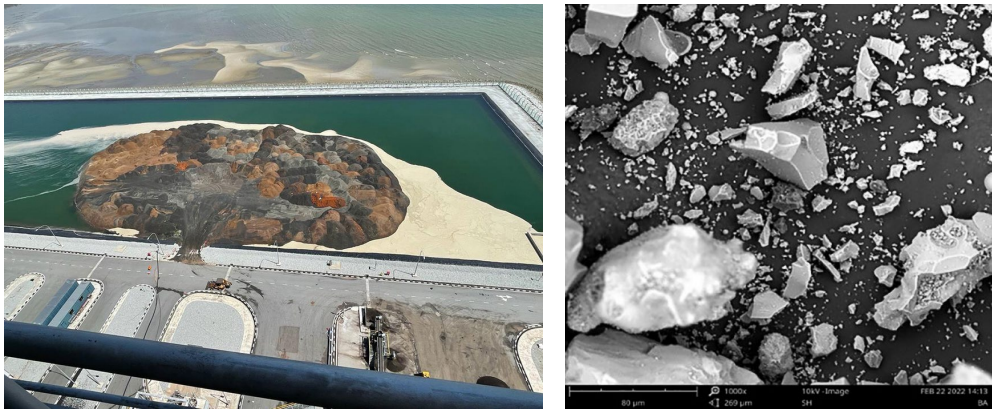

Figure 1. Coal bottom ash (CBA) lagoon at Jimah power plant, Malaysia and SEM image of CBA

Table 3. Physical properties of CBA and mining sand

Property	CBA	Mining sand
Particle size (mm)	≤4.75 mm	≤4.75 mm
Specific gravity	2.21	2.61
Fineness modulus	1.67	2.32

1.3. Foaming agent

For producing lightweight foamed concrete (LFC), a foaming agent with a specific gravity of 1.10, was employed. The foaming agent and water were mixed in the foam generator with a proportion of 1:25 based on the volume required. Air pressure was induced into the foam generator to fabricate foam with a density of 50 kg/m^3.

1.4. Water

Portable tap water was utilized for producing LFC. The water-to-cement ratio (w/c) and the water-to-sand ratio (w/s) were adjusted to obtain the least consistency of mortar based on ASTM C270-14 (ASTM, 2014e).

1.5. Mixture proportions

The replacement of the sand was based on the specific gravities of mining sand and CBA to produce the same paste volume LFC specimens. In this study, the mining sand was replaced with the CBA fine aggregate at replacement ratios of 0%, 25%, 50%, 75%, and 100% by volume. To this end, the volume of the mining sand was calculated using its specific gravity and then replaced with CBA having the same volume. Three different sizes of fine aggregates, namely less than 4.75 mm, below 2.36 mm, and less than 0.6 mm, were considered. This was to investigate the effects of fine aggregates size on the mechanical performance of LFC. Table 4 presents the proportions for all the mixtures with various CBA replacement ratios and fine aggregate sizes. NFC and FCBA mixes denote the control mortars and mortars containing fine CBA, respectively. The cement content was fixed at 522 kg/m^3 and the parameter w/c ratio was taken as 0.45. The densities of mixtures were kept in the range of ± 50 difference corresponding to the target density of 1300 kg/m^3.

Table 4. Mix proportion

Group	Mix designation	Max size of fine aggregates (mm)	CBA replacement ratio (%)	CBA (kg/m^3)	Cement (kg/m^3)	Free water (L/m^3)	w/c ratio	Sand (kg/m^3)	Foam (kg/m^3)
I	NFC-4.75	4.75	0	0	522	235	0.45	522	21
	25FCBA-4.75		25	130.5	522	235	0.45	391.5	21
	50FCBA-4.75		50	261	522	235	0.45	261	21
	75FCBA-4.75		75	391.5	522	235	0.45	130.5	21
	100FCBA-4.75		100	522	522	235	0.45	0	21
II	NFC-2.36	2.36	0	0	522	235	0.45	522	21
	25FCBA-2.36		25	130.5	522	235	0.45	391.5	21
	50FCBA-2.36		50	261	522	235	0.45	261	21
	75FCBA-2.36		75	391.5	522	235	0.45	130.5	21
	100FCBA-2.36		100	522	522	235	0.45	0	21
II	NFC-0.6	0.6	0	0	522	235	0.45	522	21
	25FCBA-0.6		25	130.5	522	235	0.45	391.5	21
	50FCBA-0.6		50	261	522	235	0.45	261	21
	75FCBA-0.6		75	391.5	522	235	0.45	130.5	21
	100FCBA-0.6		100	522	522	235	0.45	0	21

1.6. Casting and curing of samples

The same mixing method process was conducted for preparing all the mixes. As discussed before, the fresh density of LFC was taken as 1300 ± 50 kg/m^3. The total employed mining sand in the control specimens was 522 kg/m^3, which was then replaced by 25%, 50%, 75%, and 100% CBA by volume. For preparing the specimens, the cement and fine aggregate were first mixed for about three minutes using the dry mixing method. Next, water was added to the obtained homogenous mixtures, and the mixing process was continued for another three minutes. Finally, the required amount of foam was added to the mixtures to obtain the designed target density. After the mortar and foam were mixed thoroughly, the density and workability of the mixtures were measured to assure their consistency. The pan mixer with a mixing speed of 50 rev/min was used for mixing specimens. Depending on the tests performed, LFC was filled in the required steel molds. The vibrating table was used for compacting the mixtures as per BS 1881-125:1986 (British Standards Institution, 1986). All the molds were covered with plastic films and left at the ambient temperature of the laboratory (23 °C ± 1) for 24 h. The specimens were then de-molded and were cured inside the water tank at 21 °C ± 1 up to a defined age of the experiment. The hardened mechanical properties of each mixture were taken as the average of three specimens having the same mixture proportion.

2. Test procedures

2.1. Mechanical properties

Three parameters, including the compressive strength $\left(f_c^{'}\right)$, modulus of elasticity (E), and splitting tensile strength $\left(f_t^{'}\right)$, were determined for examining the effects of replacing natural fine aggregates with CBA in the LFC.

2.1.1. Compressive strength

Three 100 – mm cubes were tested to obtained the compressive strength of each LFC sample at the ages of 7- and 28- day as per EN 12390-3:2019 (European Committee for Standardization, 2019). The compressive strength was determined using compressive strength machine with the maximum capacity of 300 kN at a space rate of 0.30 kN/s. Compressive strength was defined by dividing the failure load (P) induced on the specimen by the cube cross-sectional area (A), as follows:

$$f_c^{'} = \frac{P}{A}. \tag{1}$$

The compressive strength of each specimen was taken as an average of three values. The difference between the compressive strength of each specimen with the average compressive strength was less than 10%.

2.1.2. Splitting tensile strength

The splitting tensile strength test was conducted by imposing the axial load on Ø100×200 mm cylindrical specimens at the age of 28 days, based on ASTM C496-11 (ASTM, 2011). The splitting tensile strength $\left(f_t^{'}\right)$ is governed by:

$$f_t^{'} = \frac{2P}{\pi L d}, \tag{2}$$

where the term P is the failure load, L denotes the average length of the specimen, and d is the average diameter of the specimen.

2.1.3. Modulus of elasticity (MOE)

Strain measuring tools and compression testing machines were used for finding the modulus of elasticity (MOE) of specimens, according to ASTM C469/C469M-14 (ASTM, 2014f). Based on Hooke's Law, stress is directly proportional to strain, as follows:

$$\sigma = E\varepsilon, \tag{3}$$

in which σ (MPa) represents stress, E (MPa) is the modulus of elasticity, and ε is the strain.

2.2. Water absorption

The water absorption test was performed to assess the quantity of water that the specimens could absorb under specific conditions based on their porosities. The test was conducted by concrete cube specimens measuring 100×100×100 mm in line with ASTM C642-13 (ASTM, 2013c), at the age of 28 days. Specimens were oven-dried at 105 ± 5 °C for at least two days until achieving a stable weight. The samples were soaked in water to allow sorption to continue until saturation, at which point they were cooled to room temperature. The water absorption of specimens was determined using the following equation:

$$\text{Water absorption} = \frac{\left(W_s - W_d\right)}{W_s} \times 100\%, \tag{4}$$

in which W_s and W_d are the mass of the oven-dried specimen in air and the mass of the surface-dry specimen in ambient temperature after immersion, respectively.

2.3. Ultrasonic pulse velocity

Prior to performing the compressive strength test, the Ultrasonic pulse velocity (UPV) test was performed on 100 mm cube specimens at the ages of 7- and 28-days to evaluate the quality of concrete, in accordance with ASTM C597-09 (ASTM, 2009). UPV test can provide valuable information regarding the quality of the concrete, such as consistency, cracks, cavities, and deficiencies. The traveling time for a pulse between the ends of samples was measured using a portable ultrasonic non-destructive digital indicating tester with adjoining transducers. The pulse velocity of a material is determined by its elastic characteristics and density, which are linked to the concrete's compressive strength and quality. It is simple to use, and the results are immediate.

2.4. Microstructure analysis

2.4.1. Scanning Electron Microscopy analysis

Scanning Electron Microscope (SEM) was conducted as part of this investigation. The specimens for the SEM tests were collected form the lightweight foamed concrete specimens of sand sizes 4.75, 2.36 and 0.6 mm for all the CBA sand replacement (0%, 25%, 50%, 75% and 100%).

2.4.2. X-ray diffraction

In order to study the effect of foam in the mortar, X-ray diffraction test was performed for the mixes of 100% mining sand without foam and with foam.

3. Results and discussion

3.1. Density

The fresh density and oven-dry density (ODD), saturated density, and ambient density of LFC with CBA as sand replacement are shown in Table 5. Because of the water saturation inside the concrete pores, the saturated density of specimens was generally larger than the fresh and target densities, as shown in Table 5. As a result, the oven-dry density (ODD) is often regarded as a stable amount for the purpose of design or density. The ODDs were in the range of 1092–1247 kg/m^3 for LFC specimens with sand size below 4.75 mm. For LFC specimens cast with sand sizes smaller than 2.75 mm, the ODDs were between 1008–1190 kg/m^3. The values of ODD for LFC specimens with sand sizes smaller than 0.6 mm were in the range of 1032–1332 kg/m^3. As shown in Table 5, for group one specimens, the greatest densities were obtained for specimen 25FCBA-4.75, in which the fresh density and ODD were found to be 6.19% and 7.31% greater than the control specimen NFC-4.75, respectively. The 50FCBA-2.36 specimen showed the highest density values among the second group samples with a 4.30% increase in fresh density and 180.6% in ODD compared to NFC-2.36 control concrete. Concerning LFC mixtures cast with the sieve size of smaller than 0.6 mm, replacing 100% of mining sand volume with CBA particles led to a 15.91% and 17.67% increase in fresh density and ODD of the control specimen NFC-0.6, which were the greatest than other specimens from the same group.

Table 5. Density of specimens (kg/m^3)

Mix designation	Density (kg/m^3)				
	Target	Fresh	Oven-dry	Ambient	Saturated
NFC-4.75	1300	1293	1162	1248	1449
25FCBA-4.75		1373	1247	1336	1555
50FCBA-4.75		1342	1200	1251	1470
75FCBA-4.75		1350	1092	1302	1529
100FCBA-4.75		1280	1210	1240	1502
NFC-2.36	1300	1280	1008	1137	1409
25FCBA-2.36		1270	1169	1216	1440
50FCBA-2.36		1335	1190	1234	1337
75FCBA-2.36		1298	1142	1177	1319
100FCBA-2.36		1249	1074	1100	1194
NFC-0.6	1300	1276	1132	1221	1300
25FCBA-0.6		1220	1032	1037	1159
50FCBA-0.6		1265	1138	1148	1367
75FCBA-0.6		1312	1137	1162	1376
100FCBA-0.6		1479	1332	1369	1540

3.2. Workability

Fresh concrete's workability is a multi-faceted issue that comprises a variety of compatibility, stability, and mobility needs. The use of industrial by-products in LFC as a whole or partial replacement for sand by CBA may influence the mix's fresh concrete characteristics. Slump is a metric to determine the consistency or workability of a concrete mix. The flowability of LFC specimens incorporating different CBA replacement ratios of 0%, 25%, 50%, 75%, and 100% having different sand sizes is presented in Figure 2. Figure 3 is showing the flow table set up. It can be observed from the results that regardless of the size of the fine aggregates, an increase in levels of sand replacement by CBA led to a significant reduction in slump values of mixtures. Slump values of specimens 25FCBA-4.75, 50FCBA-4.75, 75FCBA-4.75, and 100FCBA-4.75 were decreased by 1.6%, 5.83%, 5.48% and 8.54%, respectively, when compared to the control specimen NFC-4.75. Control specimen NFC-2.36 had a slump value of around 60 mm, whereas the slump values of the specimens 25FCBA-2.36, 50FCBA-2.36, 75FCBA-2.36, and 100FCBA-2.36 were found lower than the control specimen by 1.70%, 9.10%, 7.14%, and 13.20%, respectively. The control specimen NFC-0.6 showed a slump value of 54.5 mm, whereas slump values of specimens 25FCBA-0.6, 50FCBA-0.6, 75FCBA-0.6, and 100FCBA-0.6 were reduced by 2.83%, 15.95%, 11.22%, and 21.11%, respectively, compared to the control specimen. Replacing mining sand with CBA fine aggregates improves the texture of the concrete by adding more irregular and fine-shaped porous particles to the mix, which are often quite rough. Accordingly, it increases the inter-particle friction that obstructs the flow of fresh concrete. Replacing mining sand with CBA fine aggregates improves the texture of the concrete by adding more irregular and fine-shaped porous particles to the mix, which are often quite rough. Accordingly, it increases the inter-particle friction that obstructs the flow of fresh concrete. As a result, increasing the use of CBA as a replacement for mining sand lowers the workability of concrete for fixed w/c. These findings are similar to those of Singh and Siddique (2014). Rafieizonooz et al. (2016) found a similar pattern, with concrete containing CBA having lower workability.

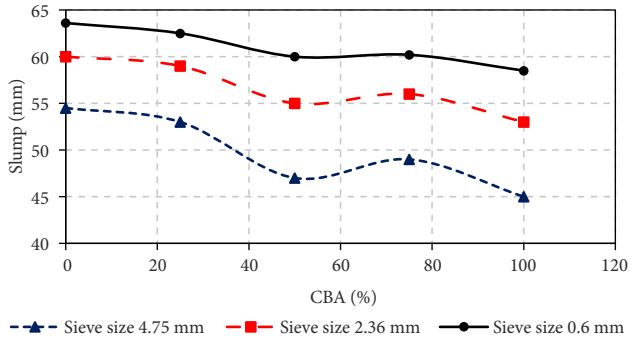

Figure 2. Influence of fine aggregate size and CBA replacement ratio on the workability of LFC

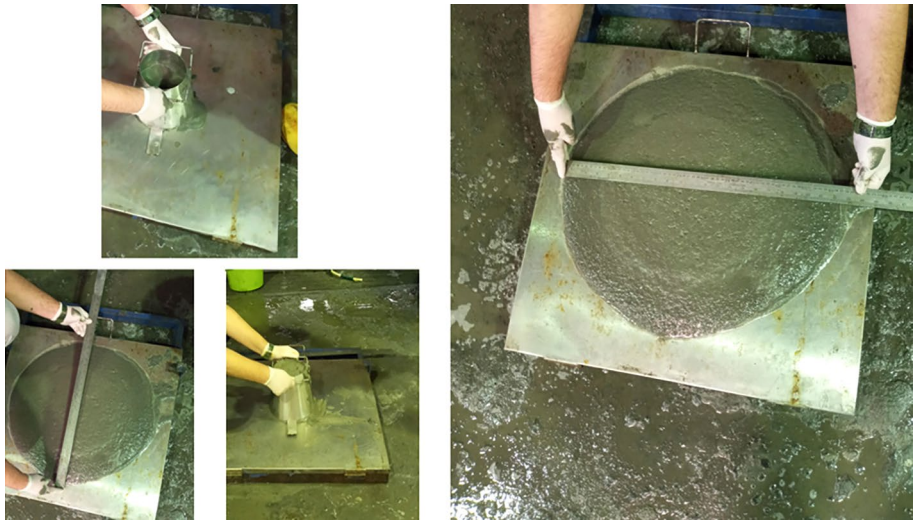

Figure 3. The flow table test setup and test

Another consideration is the impact of the size of fine particles on the workability of LFC. Regardless of CBA content, the flow test results were reduced by lowering the fine aggregate size, as shown in Figure 2. When the fine aggregate size was lowered from 4.75 mm to 2.36 mm and 0.6 mm, the slump value decreased from 64 mm to 60 mm and 55 mm, respectively. The explanation for this might be the impact of fine aggregate shape, specific surface area, and gradation on workability. By increasing the aggregate size, the small particle content and total specific surface area of the aggregate were decreased. This decreased the cement mortar adhered around the aggregate. Consequently, the slump of the mixture was increased by increasing the aggregate size (Elsharief et al., 2005; Kabir et al., 2017).

The results presented in Figure 2 indicate that the intensity of replacing mining sand with CBA on reducing the workability was reduced by increasing the aggregate size. When 100% of the mining sand was replaced with CBA, the flow of the control specimen with a sand size of 4.75 mm was observed to decrease by less than 8.5%. In contrast, the same CBA replacement ratio in the specimen cast with 0.6 mm mining sand decreased workability by more than 21%. This might be ascribed to the cumulative influence of fine aggregate size and CBA replacement ratio on LFC flowability.

3.3. Compressive strength development

The LFC compressive strength of all CBA replacement levels for 7- and 28-day curing periods and both curing methods are shown in Table 6. Besides, the relationship between the compressive strength and oven-dry density of specimens is given in Figure 4. As shown in Table 6, specimens cured in the water presented higher compressive strengths than their counterparts cured in the ambient conditions. Additionally, the compressive strength development pattern of CBA concrete with the curing period was similar to that of control concrete. The 7-day compressive strengths of water-cured specimens 25FCBA-4.75, 50FCBA-4.75, 75FCBA-4.75, and 100FCBA-4.75 were 83.63%, 77.10%, 84.21%, and 76.32% of their 28-day compressive strengths, respectively, whereas, at the curing age of 7 days, the control mixture NFC-4.75 gained 63.64% of its 28-day compressive strength. The same relationship can be observed between the 7-day-to-28-day compressive strength ratio of LFCs cast with fine aggregate sizes smaller than 2.36 mm and smaller than 0.6 mm. Water-cured specimens 25FCBA-2.36, 50FCBA-2.36, 75FCBA-2.36, and 100FCBA-2.36 at the age of 7 days could achieve 95.65%, 80.55%, 78.80%, and 69.60% of their 28-day compressive strengths, respectively, whereas, at the curing age of 7 days, the control mixture NFC-2.36 gained 71.42% of its 28-day compressive strength. Water-cured specimens 25FCBA-0.6, 50FCBA-0.6, 75FCBA-0.6, and 100FCBA-0.6 at the age of 7 days could achieve 57.14%, 80.34%, 90.14%, and 81.34% of their 28-day compressive strengths, respectively, whereas, at the curing age of 7 days, the control mixture NFC-2.36 gained 66.67% of its 28-day compressive strength. Accordingly, it can be concluded from the results achieved for the effect of CBA replacement ratio on the 7-day to 28-day compressive strength of LFC that replacing mining sand with CBA fine particles could improve the initial strength development of concrete.

There was an increase in compressive strength when CBA fine particles were used in place of mining sand, as shown in Table 6 and Figure 4. However, the influence of the CBA replacement ratio on compressive strength varies according to the size of the fine aggregate used in the concrete. It can be observed from Figures 4a and 4b that the compressive strength of specimens was increased initially by increasing the CBA replacement ratio, then gradually decreased. As shown in Figure 4a, replacing 25%, 50%, 75%, and 100% of mining sand with the sieve size of smaller than 4.75 mm with CBA fine aggregates increased the compressive strength of the control specimen from 3.3 MPa to 5.5 MPa, 4.8 MPa, 3.8 MPa, and 3.8 MPa, respectively. Likewise, when mining sand aggregate with

the sieve size of smaller than 2.36 mm was replaced with 25%, 50%, 75%, and 100% CBA fine aggregates, the compressive strength was increased from 1.65 MPa to 2.3 MPa, 3.6 MPa, 3.3 MPa, and 2.3 MPa, respectively. The significant difference in compressive strengths between specimens 25FCBA-4.75 and 50FCBA-2.36 and their corresponding control specimens could be attributed to additional pozzolanic reactions from CBA fine aggregates, which increased this unexpected improvement in bonding strength between particles (Ghadzali et al., 2020). Hence, it can be stated based on the finding of the current investigation that the optimum replacement ratios of CBA fine aggregates for the sieve sizes smaller than 4.75 mm and smaller than 2.36 mm were 25% and 50% of volume sand, respectively to lead to the greatest compressive strength in this research. The reduction in the intensity of improving the compressive strength of specimens NFC-4.75 and NFC.2.36 for CBA replacement ratios beyond 25% and 50% could be because of the constant amount of the w/c ratio used in the current study. As discussed before, CBA fine aggregates have a higher water absorption than rive sand aggregates. The high-water absorption of CBA aggregates led to a reduction in the hydration process, making the cement not act efficiently as a binder component because of a lack of water. Consequently, more water was required to continue the strength improvement of the specimen by replacing sand volume with CBA aggregates. The test results of this research are consistent with those reported in previous investigations (Balasubramaniam & Thirugnanam, 2015; Muthusamy et al., 2021). Similar to LFCs with sieve sizes smaller than 4.75 mm and smaller than 2.36 mm, the compressive strength of LFC with the fine aggregates smaller than 0.6 mm was increased by replacing mining sand with CBA particles. However, the rate of strength enhancement increased steadily when the CBA replacement ratio increased, as opposed to the previous specimens, as shown in Figure 4c. Accordingly, the optimum mining sand volume replacement ratio with CBA particles when the sieve size was smaller than 0.6 mm was found to be 100%.

As shown in Figure 4, in general, replacing mining sand volume with CBA fine aggregates increased the density of specimens. Besides, a direct relationship can be

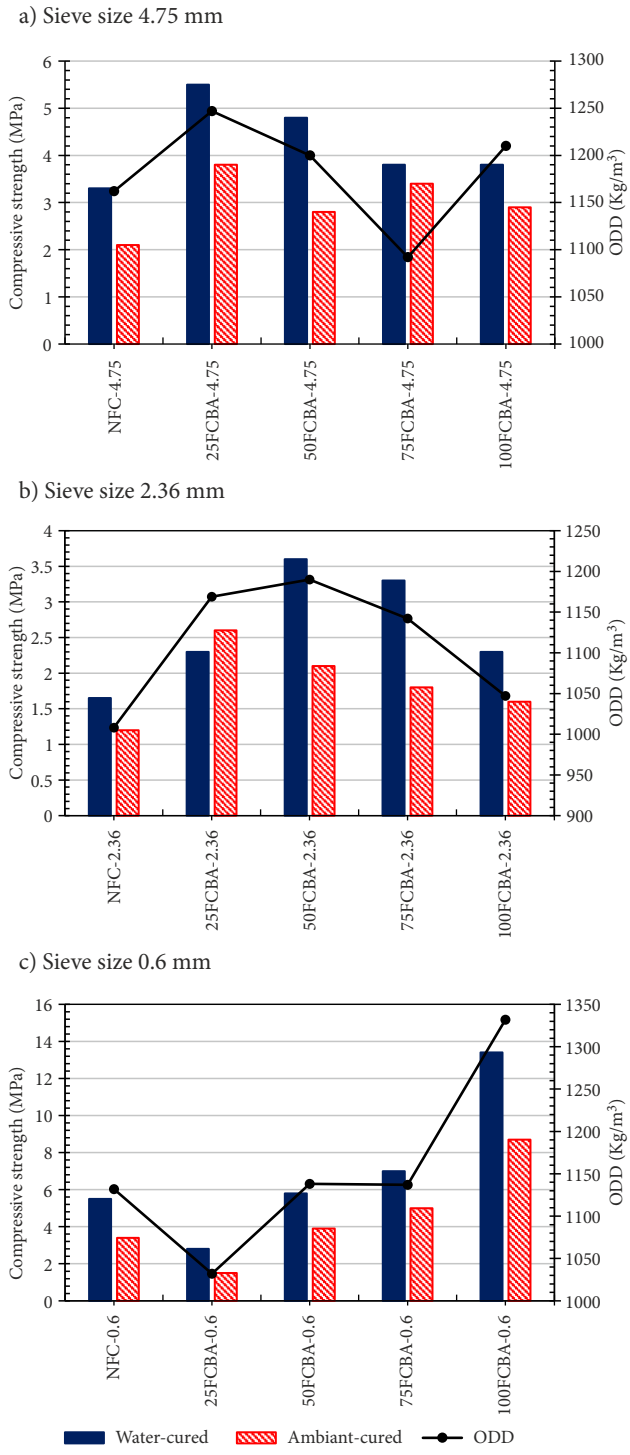

Figure 4. Relationship of the compressive strength and oven-dry density of LFC specimens

Table 6. Compressive strength of 7- and 28-day for both curing conditions

Mix designation	Compressive strength, MPa (7-day)		Compressive strength, MPa (28-day)	
	Water	Ambient	Water	Ambient
NFC	2.1	1.8	3.3	2.1
25FCBA-4.75	4.6	3.8	5.5	3.8
50FCBA-4.75	3.7	3.0	4.8	2.8
75FCBA-4.75	3.2	3.2	3.8	3.4
100FCBA-4.75	2.9	3.0	3.8	2.9
NFC-2.36	2.0	1.9	1.6	1.2
25FCBA-2.36	2.2	2.4	2.3	2.6
50FCBA-2.36	2.9	2.3	3.6	2.1
75FCBA-2.36	2.6	2.2	3.3	1.8
100FCBA-2.36	1.6	1.6	2.3	1.6
NFC-0.6	3.2	3.0	5.5	3.4
25FCBA-0.6	1.6	1.5	2.8	1.5
50FCBA-0.6	6.5	3.7	4.6	3.8
75FCBA-0.6	7.3	5.1	7.0	5.0
100FCBA-0.6	10.9	9.0	13.4	8.7

found between the compressive strength of LFC with its density. Researchers have previously reported on the favorable effect of pozzolanic reaction by coal bottom ash on the densification of concrete internal structure (Madhkhan & Katirai, 2019; Muthusamy et al., 2021). Cheriaf et al. (1999) reported that CBA particles show a low pozzolanic activity during the first two weeks of curing age. By contrast, they react with calcium hydroxide after two weeks of the curing period, generating C-S-H gel and needles. Furthermore, cement hydration generates alkali calcium hydroxide, which interacts with the reactive silica in CBA particles to form calcium silicate and aluminate hydrates. Increasing the curing age and CBA replacement ratio results in a higher quantity of calcium silicate and aluminate hydrates. As a result, the produced calcium silicate and aluminate hydrates would fill the voids in the interfacial transition zone, resulting in enhanced compressive strength. The developed pozzolanic activity of CBA fine aggregates may have negated the impacts of variables that lower the compressive strength of mixes, such as porosity, after 14 days of curing age. The pozzolanic action of CBA later neutralized the lowering components, increasing the compressive strength of the mixes.

3.4. Splitting tensile strength

The 28-day splitting tensile strength results of LFC mixtures with 50% and 100% CBA replacement ratios are presented in Figure 5. The test results show that the splitting tensile stress followed the same pattern as compressive strength. For the specimen cast with the sieve size smaller than 4.75 mm, the splitting tensile strength was increased from the control specimen NFC-4.75 to 50FCBA-4.75 and 100FCBA-4.75 as 56.47% and 38.34%, respectively. Similarly, replacing 50% and 100% mining sand volume with CBA fine particles in the control specimen with the fine aggregates smaller than 2.36 mm increased its tensile strength by 18.34% and nearly 15%, respectively. Likewise, the inclusion of CBA in the control specimen cast with the sieve size smaller than 0.6 mm led to enhancing its splitting tensile strength. However, the rate of strength increment was remarkably higher than the previous samples. As shown in Figure 5, the splitting tensile strength of the control specimen NFC-0.6 was found to be 0.77 MPa, which was increased to 0.77 MPa and approximately 1.5 MPa by substituting 50% and 100% of mining sand aggregates volume with CBA particles, respectively. The most prominent influence of replacing mining sand with CBA fine aggregates was observed when the entire mining sand aggregates with the sieve size of smaller than 0.6 mm were replaced with CBA particles. This was comparable to the impact of replacing mining sand with CBA on the compressive strength of LFC described earlier. The results of the incorporation of CBA in LFC on the splitting tensile strength were in good agreement with the ones reported by Singh and Siddique (2014) and Aggarwal and Siddique (2014). In general, the splitting tensile strength of LFC is influenced by the paste quality and the compressive strength. However, the influence of the former is more than the latter. Fine aggregate characteristics also have an impact on the concrete's paste quality and interfacial transition zone, influencing the tensile strength (Singh & Siddique, 2014). The performance of tensile strength owing to the inclusion of CBA in the concrete mix may be an indicator of C-S-H gel formation. The pozzolanic reaction helped to enhance the amount of C-S-H gel produced by the hydration process, which improved aggregate bonding and made high-strength concrete stronger and denser (Ghafoori & Bucholc, 1997).

The relationship between the compressive strength and tensile strength of LFC having CBA as fine aggregates is presented in Figure 6. According to the test results, the following equation is proposed for predicting the tensile strength of LFC with CBA as fine aggregates:

$$f_t' = 0.2515\left(f_c'\right)^{0.67}. \quad (5)$$

The acceptable correlation of the proposed equation indicates that it can be used for calculating the splitting tensile strength of LFC including CBA as fine aggregates with respect to the compressive strength. The model derived from the current investigation's test findings is similar to the CEB-FIP code for concrete buildings (Comite Euro-International Du Beton, 1990) equation $f_t' = 0.30\left(f_{cyl}'\right)^{\frac{2}{3}}$, where $f_{cyl}' = 0.8 f_{cu}'$.

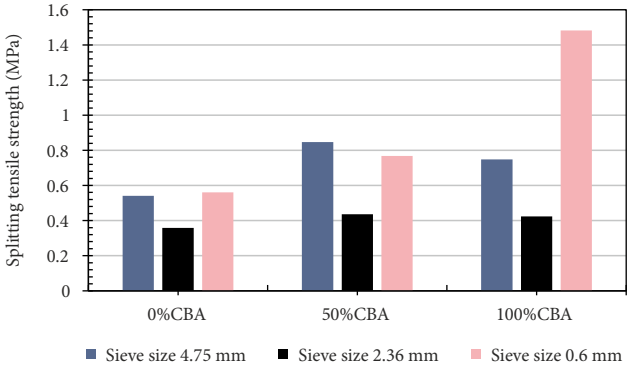

Figure 5. Influence of CBA replacement ratio on the splitting tensile strength of LFC

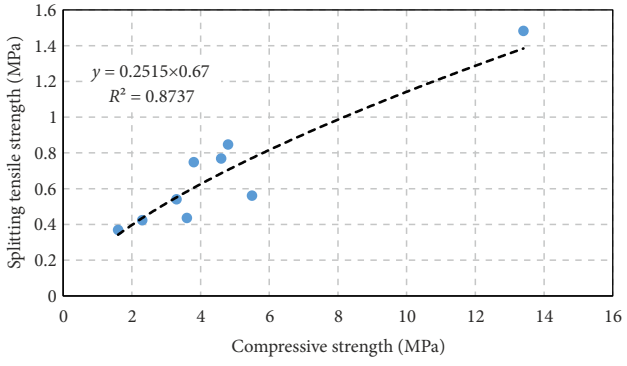

Figure 6. Relation between compressive strength and splitting tensile strength of LFC containing CBA

3.5. Modulus of elasticity

Modulus of elasticity of LFC mixtures with 50% and 100% CBA replacement ratios was achieved at the curing age of 28-day. The test results are displayed in Figure 7. It was found that the modulus of elasticity of specimens cast with the sieve size of smaller than 4.75 mm and smaller than 0.6 mm increased in accordance with an increase of replacement of mining sand aggregates with CBA fine aggregates. The modulus of elasticity of control specimen NFC-4.75 was almost 4.2 GPa. When 50% and 100% of mining sand was substituted with CBA, elastic modulus of NFC-4.75 increased to 4.23 GPa and 13.33 GPa, respectively. The modulus of elasticity of LFC containing 50% and 100% CBA of smaller than 0.6 was 6.6 GPa and 16 GPa, respectively which were remarkably higher than the corresponding control specimen NFC-0.6 with the elastic modulus of 4.2 GPa. Contrary to the previous cases, replacing 50% and 100% of mining sand with the sieve size of smaller than 2.36 reduced the elastic modulus of control mixture NFC-2.36 to 1.05 GPa and 2.5 GPa, respectively. As shown in Figure 7, the modulus of elasticity has a direct relationship with ODD. This finding was confirmed by Kozłowski and Kadela (2018), who observed that the modulus of elasticity of foamed concrete was increased with an increase in its density.

3.6. Ultrasonic pulse velocity

Table 7 displays the ultrasonic pulse velocity (UPV) findings for specimens cured under ambient and water conditions at 7- and 28-day ages. It can be observed from Table 7 that regardless of CBA content, increasing the curing age increased the UPV values. Furthermore, LFCs cured in the water had greater UPV values than those cured in ambient circumstances. This was attributable to enhanced pore structure and lower porosity as a result of increased cement hydration reaction with no moisture loss from the concrete sample. When 25% of the mining sand volume was replaced with CBA fine aggregates, the UPV values were lower than the control mixture. For example, after 28 days of curing, the UPV values of the water-cured LFC mixes 25FCBA-4.75, 25FCBA-2.36, and 25FCBA-0.6 were reduced by 7.60%, 5.10%, and 5.69%, respectively, compared to their corresponding control mixtures. In contrast, replacing 50% or 75% of the mining sand with CBA fine aggregates improved the UPV values of mixes compared to respective control specimens. For example, after a 28-day curing period, the UPV values of the water-cured LFC combinations 50FCBA-4.75, 50FCBA-2.36, and 50FCBA-0.6 were increased by 10.40%, 23.53%, and 30.25%, respectively, in comparison to their corresponding control mixtures. At the same curing age, the UPV values for the water-cured LFC mixes 75FCBA-4.75, 75FCBA-2.36, and 75FCBA-0.6 were higher by 12.40%, 9.01%, and 32.74%, respectively, than for the control mixtures. When 100% of the volume of mining sand is replaced with CBA fine aggregates, a similar trend is seen. However, the intensity of the 100% CBA replacement ratio on increasing the UPV values of the control mixes was lower when compared to the 50% and 75% CBA replacement ratios. Higher pulse velocities of LFC specimens with CBA than the control ones might be due to a substantial reduction in permeable pore space. Almost the same results were observed

Table 7. UPV through LFC mixtures

Mix designation	UPV 7-day (km/s)		UPV 28- day (km/s)	
	Ambient	Water	Ambient	Water
NFC	1.85	2.05	2.10	2.50
25FCBA-4.75	1.66	1.98	2.08	2.31
50FCBA-4.75	2.05	2.37	2.21	2.76
75FCBA-4.75	2.24	2.52	2.38	2.81
100FCBA-4.75	2.27	2.44	2.26	2.64
NFC-2.36	2.17	2.34	2.19	2.55
25FCBA-2.36	2.03	2.26	2.11	2.42
50FCBA-2.36	2.22	2.46	2.25	2.56
75FCBA-2.36	2.31	2.58	2.36	2.78
100FCBA-2.36	1.88	2.15	1.92	2.25
NFC-0.6	2.03	2.30	2.23	2.81
25FCBA-0.6	1.80	2.06	1.78	2.65
50FCBA-0.6	2.41	2.65	3.18	3.66
75FCBA-0.6	2.64	3.11	3.35	3.88
100FCBA-0.6	2.44	2.78	2.98	4.55

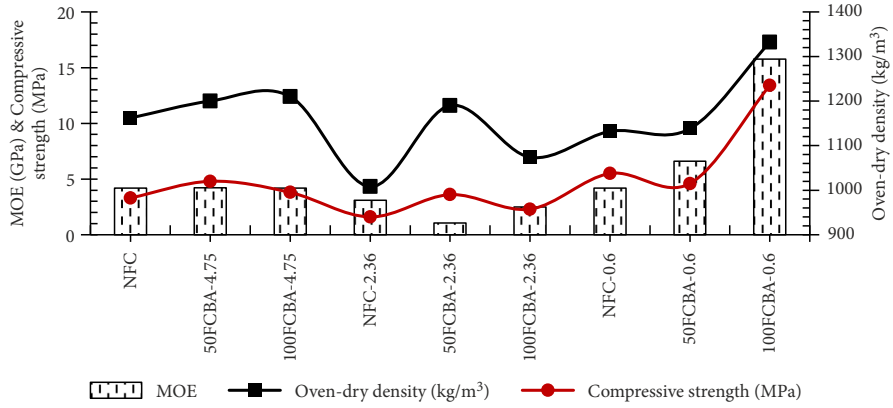

Figure 7. Relationship between modulus of elasticity and compressive strength of LFC with CBA replacement ratio and ODD

by Rafieizonooz et al. (2016) who reported that for any curing age, UPV values of concrete at low replacement ratios of CBA fine aggregates were less than the control concrete, whereas at high replacement ratios, the UPV values for concrete were increased compared to that of control mixtures.

Concerning the influence of the fine aggregate sieve size on UPV results, it can be noticed from the results that, in general, using finer aggregates could increase the UPV values for both control mixtures and specimens with CBA fine aggregates. For instance, the UPV test result of the water-cured control mixture with 4.75 mm sieve size was found to be 2.5, whereas it was increased by 2.0% and 12.4% when sieve sizes of 2.36 mm and 0.6 mm were used. The same trend can be observed when finer CBA aggregates were used in LFCs. This tendency may be related to the improved filling ability of finer particles (Lim et al., 2013). Larger aggregates were less uniform than smaller aggregates. Therefore, the pores on the surface and interior of the specimens made with larger aggregates were greater than those made with smaller aggregates. As defined by Neville and Brooks (2010), concrete having UPV values ranging from 3.66 km/s to 4.58 km/s is classified as "good quality". In general, the UPV of mixes in which at least 50% of the 0.6 mm sand was replaced with CBA fine aggregates have good quality.

The relationship between compressive strength and UPV of mixtures obtained in the current research is shown in Figure 8. According to Figure 8, the UPV value is directly proportional to the concrete strength. The UPV values obtained were in agreement with the mixes' oven-dry density, as shown in Table 7. As a result, increasing concrete density improves both the UPV value and the concrete compressive strength. Based on the results, Eqn (5) can be used to predict the cube compressive strength according to the corresponding UPV value. The coefficient determination of $R^2 = 0.7508$ shows good relevance between the results and the regression curve:

$$f_{cu} = 0.35e^{(0.88UPV)}, \quad (5)$$

in which f_{cu} denotes the cube compressive strength (MPa) and UPV is the transverse ultrasonic pulse velocity (km/s).

3.7. Water absorption and porosity

Water absorption test results of CBA concrete mixtures are displayed in Figure 9. Besides, the ratio of water absorbed by CBA concrete mixes to control concrete specimens ($WA_{CBA}/WA_{cont.}$), compressive strength, and ODD of concrete mixtures at the curing period of 28-day are given in Table 8. Regardless of the CBA replacement ratio, replacing mining sand with the sieve size smaller than 4.75 mm increased the water absorption of LFCs compared with the control concrete NFC-4.75, as shown in Figure 9. Water absorption was shown to increase with an increase in CBA replacement ratio up to 75% for specimens cast with fine aggregate sizes less than 4.75 mm, followed by

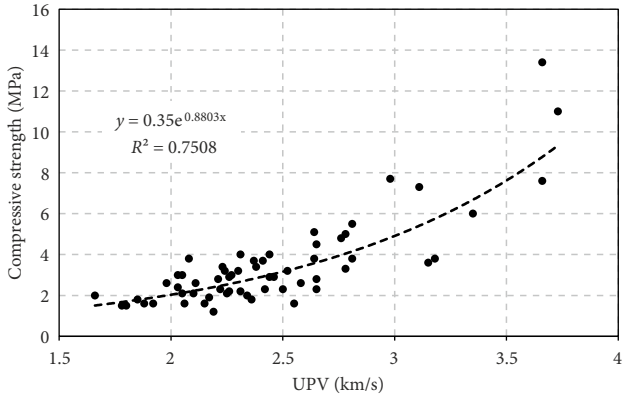

Figure 8. The relationship between the compressive strength UPV

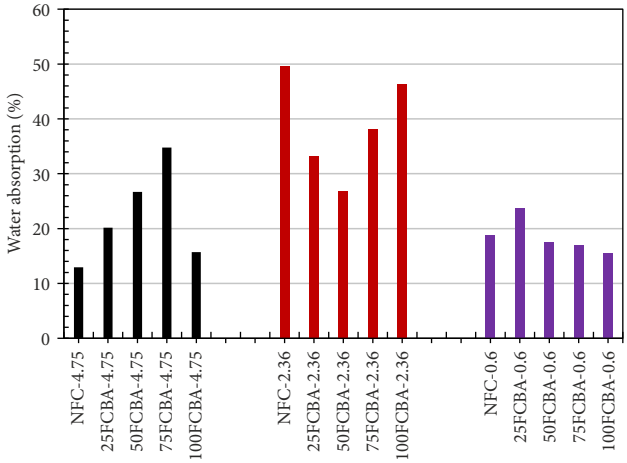

Figure 9. Variation in water absorption of LFC with CBA content

a sudden drop in 100% CBA replacement ratio. Regarding the second group specimens cast with the sieve size of smaller than 2.36, the concrete mixtures containing CBA fine particles had a lower water absorption ratio than the control specimen NFC-2.36. As shown in Figure 9, the water absorption ratio of the control specimen NFC-2.36 was reduced from 49.64% to 33.20%, 26.90%, 38.13%, and 46.28% by replacing 25%, 50%, 75%, and 100% of mining sand volume with CBA aggregates, respectively. For the third group specimens cast with the sieve size smaller than 0.6 mm, except for the specimen 25FCBA-0,6, all other CBA concrete mixtures had lower water absorption ratios than the control concrete NFC-0.6. When 25% of mining sand was replaced with CBA particles, the water absorption ratio of NFC-0.6 increased from 18.71% to 23.72%. In contrast, CBA replacement levels of 50%, 75%, and 100% resulted in water absorption ratios of 17.54%, 17.02%, and 15.60%, which were lower than the control specimen.

As shown in Table 8, the porosity of specimens 25FCBA-4.75 and 50FCBA-4.75 was lower than that of the control specimen, which was consistent with their greater ODD. In comparison, substituting 75% of the volume of mining sand with CBA particles raised the porosity of NFC-4.75 by 36.84% while decreasing its ODD by

6.07%. As indicated in Table 8, specimen 75FCBA-4.75 had the highest porosity and smallest ODD when compared to the other specimens in the same group, which corresponded to its maximum water absorption ratio. The results obtained for the influence of replacing mining sand with the sieve size smaller than 4.75 mm with CBA fine particles on the water absorption of specimens were in good agreement with the experimental work of Singh and Siddique (2014). Table 8 shows that, except for the specimen 25FCBA-2.36, the other concrete mixes had nearly the same porosity as the control specimen NFC-2.36 for the second group specimens cast with a sieve size lower than 2.36 mm. The ODD values of the CBA concrete mix, on the other hand, were greater than those of the control specimen, which might explain why they had a lower water absorption ratio than the NFC-2.36. When mining sand volume was replaced with CBA aggregates in the control specimen NFC-0.6, the porosity of the concrete was decreased. In comparison to other concrete mixes from the same group specimens, specimen 25FCBA-0.6 had the smallest ODD and, as a result, the greatest water absorption ratio.

The results obtained for the water absorption of LFCs cast with the sieve size of smaller than 4.75 mm are in good agreement with the results reported by Singh and Siddique (2014) and Siddique (2013). The cement paste pores and the interfacial transition zone (ITZ) between the cement paste and aggregates are the two ways by which water may be transported in the mortar. The type of aggregates used in the concrete might significantly impact water transportation across the ITZ. According to several studies, lightweight aggregate concrete has an ITZ that is noticeably thinner than normal concrete (Zhang & Gjørv, 1990; Elsharief et al., 2005; Kabir et al., 2017). In the case of cement paste with lightweight aggregates, the cement paste was slightly absorbed into lightweight aggregates with a porous structure and, accordingly, hydration products, such as plate-like calcium hydroxide crystals, were formed in the pores of the lightweight aggregates and merged over the ITZ (Zhang & Gjørv, 1992; Kabir et al., 2017). Furthermore, a pozzolanic interaction within lightweight aggregates and hydration products occurred, which made a denser microstructure of ITZ (Kim et al., 2012; Kabir et al., 2017). On the other hand, the water absorption of foamed concrete is generally higher than non-foamed concrete because of its lower density (Nambiar & Ramamurthy, 2007). As a result, substituting mining sand with sieve sizes less than 2.36 mm and 0.6 mm with CBA fine aggregates reduced water absorption in lightweight foamed concrete mixes.

For each set of LFCs with the considered fine aggregate size, the specimen with the lowest WA_{CBA}/WA_{cont} ratio showed the highest compressive strength. When the sieve size was less than 2.36 mm, the specimen 50FCBA-2.36, which had a WA_{CBA}/WA_{cont} ratio of 0.54, had the greatest compressive strength of 3.6 MPa when compared to other specimens in the same group. Likewise, when the sieve size was smaller than 0.6 mm, the specimen with the greatest compressive strength was 100FCBA-0.6, which had a strength of 13.4 MPa and the lowest WA_{CBA}/WA_{cont} ratio of 0.83.

3.8. Microstructure analysis

3.8.1. Scanning Electron Microscopy analysis

Scanning Electron Microscopy (SEM) images of the lightweight foamed concrete with 4.75, 2.36 and 0.6 mm containing (0%, 25%, 50%, 75% and 100%) CBA as sand replacement with a magnification factor of 200 μm and 100 μm are displayed in Figure 10 for each mix. It can be noticed that Figure 10a presents the mixes with sand size below 4.75 mm. The Figures 10b and 10c depict the mixes

Table 8. Relationship between the water absorption, compressive strength and ODD of LFC

Mix designation	Water absorption (%)	WA_{CBA}/WA_{cont}	Porosity (%)	Compressive strength (MPa)	ODD (kg/m^3)
NFC-4.75	12.96	–	57	3.3	1162
25FCBA-4.75	20.15	1.55	53	5.5	1247
50FCBA-4.75	26.70	2.06	53	4.8	1200
75FCBA-4.75	34.78	2.68	78	3.8	1092
100FCBA-4.75	15.71	1.21	56	3.8	1210
NFC-2.36	49.64	–	54	1.6	1008
25FCBA-2.36	33.20	0.67	63	2.3	1169
50FCBA-2.36	26.90	0.54	55	3.6	1190
75FCBA-2.36	38.13	0.77	55	3.3	1142
100FCBA-2.36	46.28	0.93	51	2.3	1074
NFC-0.6	18.71	–	63	5.5	1132
25FCBA-0.6	23.72	1.27	54	2.8	1032
50FCBA-0.6	17.54	0.94	52	4.6	1138
75FCBA-0.6	17.02	0.91	58	7.0	1137
100FCBA-0.6	15.60	0.83	60	13.4	1332

a) SEM for sand 4.75 mm

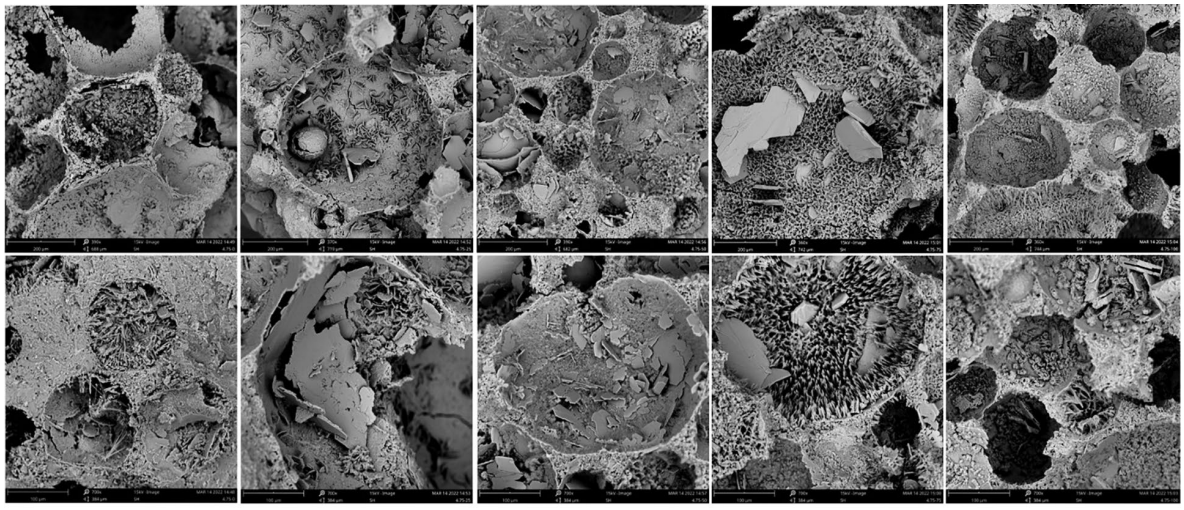

b) SEM for sand 2.36 mm

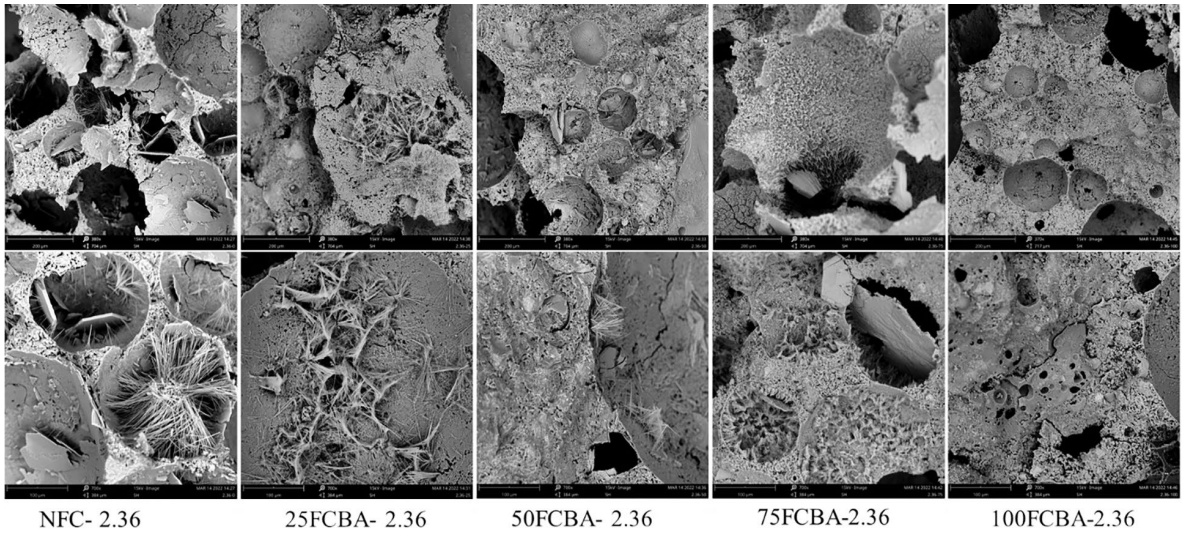

c) SEM for sand 0.6 mm

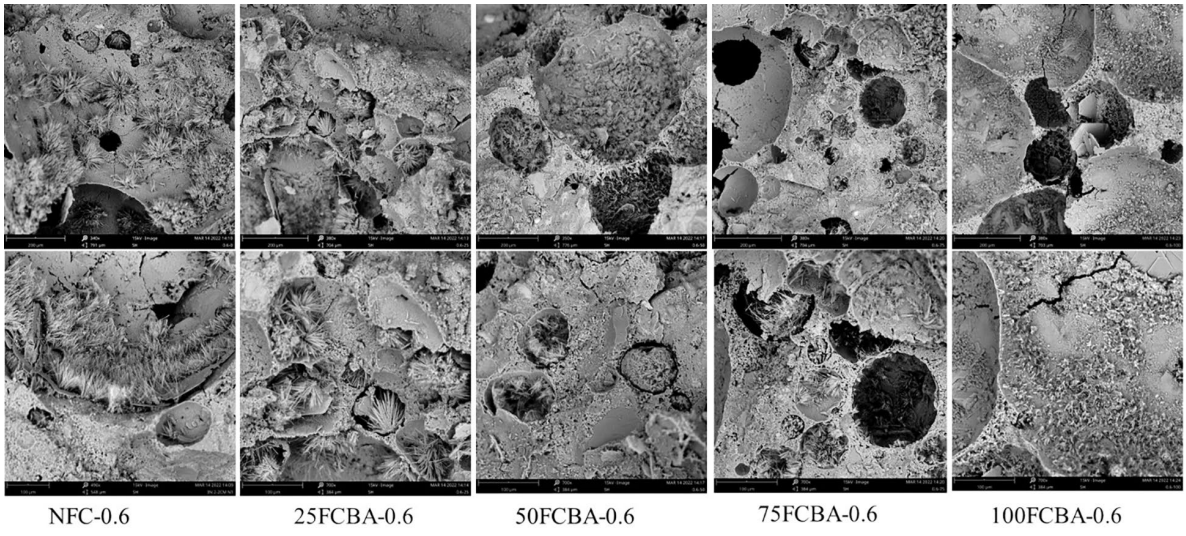

Figure 10. Scanning Electron Micrograph of lightweight foamed concrete mixtures:
a – sand 4.75 mm; b – sand 2.36 mm; and c – sand 0.6 mm

with sand sizes below 2.36 mm, and below 0.6 mm, respectively. It can be seen from Figure 10a that the interfacial zones between the matrix and the voids were thin, leading to a weak structure of the concrete. Besides, the presence of micro cracks in the matrix can be found in the SEM results of the control concrete. These observations could be attributed to the lower compressive strength of the control concrete than LFC mixtures containing CBA fine aggregates. Replacing 25% of mining sand volume with CBA particles resulted to a uniform distribution of the voids in the LFC structure, as shown in Figure 10. By contrast, a non-uniform distribution of the voids can be observed in the LFC structure when 50% of the mining sand volume was replaced with CBA particles, as displayed in Figure 10. Besides, the matrix of the LFC concrete with 50% CBA as sand replacement was more compact than previous mixtures. The SEM results of the mixes with 75% BA as sand replacement. It can be seen from Figure 10 that the size and number of the voids in the concrete were relatively less than the control concrete, as well as LFCs with 25% and 50% CBA as sand replacement. Concerning the mix with 100% CBA as sand replacement, a sintering structure can be noticed in the concrete, as shown in Figure 10. In general, the results show that the voids and micro-pores found in CBA-based foamed concrete were caused by the porous foam structures and CBA particles, respectively.

It also can be seen from the mixes with 0.6 mm size that the void structure was changed compared to the other sizes. The voids distribution of the mixes with fine aggregates of 4.75 mm size was large compared to the corresponding mixes with 0.6 mm size. Thus, the strength enhancement in the mixes with 0.6 mm size is higher. Another point that can be noticed from SEM results is the relationship between the size of the voids and the CBA replacement ratio. As shown in Figure 10, the size of the micro-voids was reduced by increasing the CBA replacement ratio. This could be attributed to the improvement in the contact area between the cementitious material and the CBA particles. Due to the high surface tension of water, cement forms a thin shell covering the components' surface, and significant reactions occur at the contact surface when sufficient compaction is introduced into the fresh concrete mix (Lee et al. 2010). As discussed before, the CBA particles have a porous structure. Accordingly, the porosity of the concrete increases with increasing the CBA content (Onprom et al., 2015).

A rough surface can be observed from the SEM results of mixtures, shown in Figure 10, which could be due to hydration products such as C-S-H gel, $Ca(OH)_2$, and ettringite. The CBA particles as sand replacement contribute to the formation of tobermorite ($Ca_5Si_6O_{16}(OH)_2{\cdot}5H_2O$), which is a calcium silicate hydrate (Galvánková et al., 2016). A greater amount of grass like C-S-H structure can also be generated by increasing the CBA replacement ratio to 100% (Li et al., 2018). These might be considered as reasons for the greater compressive strength of LFC with CBA than the control concrete with mining sand fine aggregates.

3.8.2. X-ray diffraction

The X-ray diffraction patterns of the control concrete and mortar are presented in Figure 11. The presence of portlandite, calcium hydroxide ($Ca(OH)_2$), coesite and tobermorite ($Ca_5Si_6O_{16}(OH)_2{\cdot}5H_2O$) can be found in both foamed concrete and mortar. Both the portlandite and calcium hydroxide were present at 18°, 34°, 47°, 50°, and 54° (2-Theta). The presence of costite was noticed at 26°, 29°, 32°, 39° and 45° (2-Theta). In addition, tobermorite was at 9°, 18°, 26°, 29°, 31°, 34°, 39°, 47° and 48° (2-Theta). Singh and Siddique (2015) found that C-S-H gel formed when CBA particles reacted with portlandite (Singh & Siddique, 2015). An increase in the intensity at 18° 2θ, as well as the presence of portlandite and calcium hydroxide, can be observed in Figure 11. This issue can explain the difference in the compressive strength as the portlandite did not react fully in the pozzolanic reaction to form the C-S-H gel compared to the control mortar. It was reported that a sharp peaks near 18° and 34° 2θ were presented portlandite which formed due the hydration (Hou et al., 2004). A reduction in the tobermorite peaks at 9°, 18°, 31° and 39° can be noticed when the foam was introduced which could be related to the compressive strength. An increase in the tobermorite peaks is attributed to strength enhancement (Cai et al., 2021).

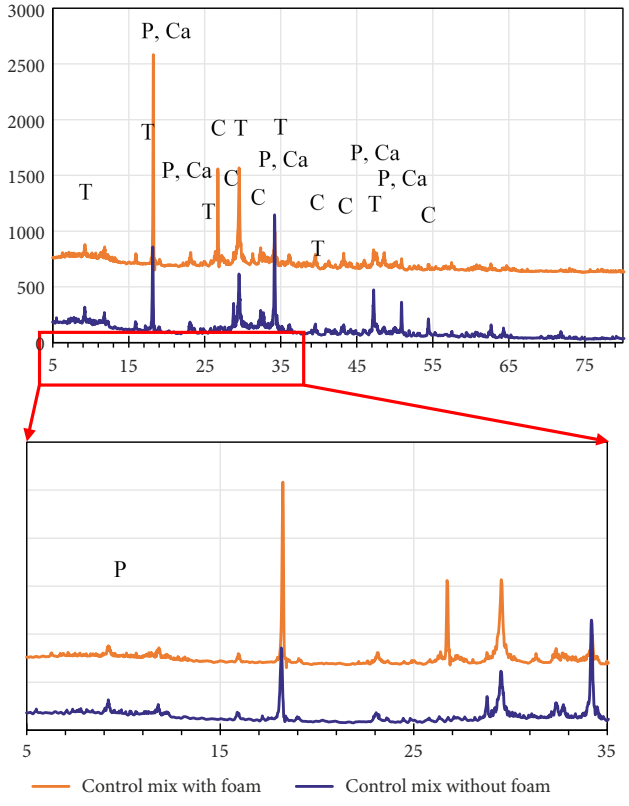

Figure 11. X-ray diffraction of the control foamed concrete and mortar; where P is portlandite, Ca is calcium hydroxide ($Ca(OH)_2$), C is coesite and T is tobermorite ($Ca_5Si_6O_{16}(OH)_2{\cdot}5H_2O$)

Conclusions

This research investigated the effects of replacing the conventional mining sand with CBA as fine aggregates on the mechanical properties of lightweight foamed concrete. The investigated parameters include flow table, mechanical properties such as compressive, flexural, and splitting tensile strengths. The water absorption and UPV were also investigated. In addition, the microstructure analyses that include SEM and XRD were conducted and reported. Based on the study, the following conclusions can be drawn:

1. The lower sand size reduces the flow values which could be attributed to the impact of fine aggregates' shape, specific surface area, and gradation on the workability.
2. The water absorption of mixes with CBA of sizes below 2.75 mm and 0.6 mm showed lower compared to the control mixes with conventional mining sand.
3. The fresh density of LFC was within the allowed range of 1300 ± 50 kg/m^3. However, the oven dry density was ranged in 1008–1332 kg/m^3.
4. Water-cured specimens produced higher compressive strength as expected; in addition, the use of smaller size rough CBA as the fine aggregates enabled better bond and hence produced higher compressive strength compared to mixes with mining sand.
5. The MOE of LFC containing 50% and 100% CBA with smaller than 0.6 were found as 6.6 GPa and 13.4 GPa, respectively; the refinement of pores in the LFC, thus produced higher than the corresponding control specimen NFC-0.6 with the elastic modulus of 4.2 GPa. The density of the concrete also plays a role in the MOE values.
6. The introduction of CBA particles with rough surfaces enhanced the bond and the particle sizes of 0.6 mm and below reduces the micro voids in the foamed concrete.
7. The reduction in the tobermorite peaks was noticed after the introduction of foam which could also be attributed to the reduction in the compressive strength.

Acknowledgements

The authors gratefully acknowledge the financial support received from University of Malaya through University of Malaya's Impact Oriented Interdisciplinary Research Grant with Project No. IIRG016C-2019.

References

Abubakar, A. U., & Baharudin, K. S. (2012). Properties of concrete using tanjung bin power plant coal bottom ash and fly ash. *International Journal of Sustainable Construction Engineering and Technology*, *3*(2), 56–69.

Aggarwal, Y., & Siddique, R. (2014). Microstructure and properties of concrete using bottom ash and waste foundry sand as partial replacement of fine aggregates. *Construction and Building Materials*, *54*, 210–223. https://doi.org/10.1016/j.conbuildmat.2013.12.051

Alnahhal, A. M., Alengaram, U. J., Yusoff, S., Singh, R., Radwan, M. K. H., & Deboucha, W. (2021). Synthesis of sustainable lightweight foamed concrete using palm oil fuel ash as a cement replacement material. *Journal of Building Engineering*, *35*, 102047. https://doi.org/10.1016/j.jobe.2020.102047

Alnahhal, A. M., Alengaram, U. J., Yusoff, S., Darvish, P., Srinivas, K., & Sumesh, M. (2022). Engineering performance of sustainable geopolymer foamed and non-foamed concretes. *Construction and Building Materials*, *316*, 125601. https://doi.org/10.1016/j.conbuildmat.2021.125601

American Society for Testing and Materials. (2009). *Standard test method for pulse velocity through concrete* (No. ASTM C597-09).

American Society for Testing and Materials. (2011). *Standard test method for splitting tensile strength of cylindrical concrete specimens* (No. ASTM C496-11).

American Society for Testing and Materials. (2013a). *Standard specification for concrete aggregates 1* (No. ASTM C33/C33M-13).

American Society for Testing and Materials. (2013b). *Standard specification for standard sand* (No. ASTM C778-13).

American Society for Testing and Materials. (2013c). *Standard test method for density, absorption, and voids in hardened concrete* (No. ASTM C642-13).

American Society for Testing and Materials. (2014a). *Standard specification for Portland Cement* (No. ASTM C150-14).

American Society for Testing and Materials. (2014b). *Standard specification for coal fly ash and raw or calcined natural pozzolan for use in concrete* (No. ASTM C618-14).

American Society for Testing and Materials. (2014c). *Standard test methods for chemical analysis of hydraulic cement* (No. ASTM C114-14).

American Society for Testing and Materials. (2014d). *Standard test method for sieve analysis of fine and coarse aggregates* (No. ASTM C136/C136M-14).

American Society for Testing and Materials. (2014e). *Standard specification for mortar for unit masonry* (No. ASTM C270-14).

American Society for Testing and Materials. (2014f). *Standard test method for static modulus of elasticity and Poisson's ratio of concrete in compression* (No. ASTM C469/C469M-14).

Argiz, C., Moragues, A., & Menéndez, E. (2018). Use of ground coal bottom ash as cement constituent in concretes exposed to chloride environments. *Journal of Cleaner Production*, *170*, 25–33. https://doi.org/10.1016/j.jclepro.2017.09.117

Aswathy, P. U., & Paul, M. M. (2015). Behaviour of self compacting concrete by partial replacement of fine aggregate with coal bottom ash. *International Journal of Innovative Research in Advanced Engineering* (*IJIRAE*), *2*(10), 45–52.

Bai, Y., Darcy, F., & Basheer, P. A. M. (2005). Strength and drying shrinkage properties of concrete containing furnace bottom ash as fine aggregate. *Construction and Building Materials*, *19*(9), 691–697. https://doi.org/10.1016/j.conbuildmat.2005.02.021

Baite, E., Messan, A., Hannawi, K., Tsobnang, F., & Prince, W. (2016). Physical and transfer properties of mortar containing coal bottom ash aggregates from Tefereyre (Niger). *Construction and Building Materials*, *125*, 919–926. https://doi.org/10.1016/j.conbuildmat.2016.08.117

Bakoshi, T., Kohno, K., Kawasaki, S., & Yamaji, N. (1998). *Strength and durability of concrete using bottom ash as replacement for fine aggregate*. American Concrete Institute, ACI Special Publication.

Balasubramaniam, T., & Thirugnanam, G. S. (2015). An experimental investigation on the mechanical properties of bottom ash concrete. *Indian Journal of Science and Technology*, *8*(10), 992–997. https://doi.org/10.17485/ijst/2015/v8i10/54307

Bohari, A. A. M., Skitmore, M., Xia, B., & Teo, M. (2017). Green oriented procurement for building projects: Preliminary findings from Malaysia. *Journal of Cleaner Production*, *148*, 690–700. https://doi.org/10.1016/j.jclepro.2017.01.141

British Standards Institution. (1986). *Testing concrete. Methods for mixing and sampling fresh concrete in the laboratory* (No. BS 1881-125:1986).

Cai, Q., Ma, B., Jiang, J., Wang, J., Shao, Z., Hu, Y., Qian, B., & Wang, L. (2021). Utilization of waste red gypsum in autoclaved aerated concrete preparation. *Construction and Building Materials*, *291*, 123376.

Cheriaf, M., Rocha, J. C., & Péra, J. (1999). Pozzolanic properties of pulverized coal combustion bottom ash. *Cement and Concrete Research*, *29*(9), 1387–1391. https://doi.org/10.1016/S0008-8846(99)00098-8

Chua, S. C., & Oh, T. H. (2010). Review on Malaysia's national energy developments: Key policies, agencies, programmes and international involvements. *Renewable and Sustainable Energy Reviews*, *14*(9), 2916–2925. https://doi.org/10.1016/j.rser.2010.07.031

Chung, S.-Y., Abd Elrahman, M., Kim, J.-S., Han, T.-S., Stephan, D., & Sikora, P. (2019). Comparison of lightweight aggregate and foamed concrete with the same density level using image-based characterizations. *Construction and Building Materials*, *211*, 988–999. https://doi.org/10.1016/j.conbuildmat.2019.03.270

Comite Euro-International Du Beton. (1990). *CEB-FIP Model code 1990: Design code*.

Elsharief, A., Cohen, M. D., & Olek, J. (2005). Influence of lightweight aggregate on the microstructure and durability of mortar. *Cement and Concrete Research*, *35*(7), 1368–1376. https://doi.org/10.1016/j.cemconres.2004.07.011

European Committee for Standardization. (2019). *Testing hardened concrete - Part 3: Compressive strength of test specimens* (No. EN 12390-3:2019).

Falliano, D., De Domenico, D., Ricciardi, G., & Gugliandolo, E. (2018). Key factors affecting the compressive strength of foamed concrete. *IOP Conference Series: Materials Science and Engineering*, *431*(6), 062009. https://doi.org/10.1088/1757-899X/431/6/062009

Farahani, H., & Bayazidi, S. (2018). Modeling the assessment of socio-economical and environmental impacts of sand mining on local communities: A case study of Villages Tatao River Bank in North-western part of Iran. *Resources Policy*, *55*, 87–95. https://doi.org/10.1016/j.resourpol.2017.11.001

Galvánková, L., Másilko, J., Solný, T., & Štěpánková, E. (2016). Tobermorite synthesis under hydrothermal conditions. *Procedia Engineering*, *151*, 100–107. https://doi.org/10.1016/j.proeng.2016.07.394

Gencel, O., Kazmi, S. M. S., Munir, M. J., Kaplan, G., Bayraktar, O. Y., Yarar, D. O., Karimipour, A., & Ahmad, M. R. (2021). Influence of bottom ash and polypropylene fibers on the physico-mechanical, durability and thermal performance of foam concrete: An experimental investigation. *Construction and Building Materials*, *306*, 124887. https://doi.org/10.1016/j.conbuildmat.2021.124887

Ghadzali, N. S., Ibrahim, M. H. W., Zuki, S. S. M., Sani, M. S. H., & Al-Fasih, M. Y. M. (2020). Material characterization and optimum usage of Coal Bottom Ash (CBA) as sand replacement in concrete. *International Journal of Integrated Engineering*, *12*(9), 9–17. https://doi.org/10.30880/ijie.2020.12.09.002

Ghafoori, N., & Bucholc, J. (1997). Properties of high-calcium dry bottom ash concrete. *ACI Materials Journal*, *94*(2), 90–101. https://doi.org/10.14359/289

Gielen, D., Boshell, F., Saygin, D., Bazilian, M. D., Wagner, N., & Gorini, R. (2019). The role of renewable energy in the global energy transformation. *Energy Strategy Reviews*, *24*, 38–50. https://doi.org/10.1016/j.esr.2019.01.006

Gursel, A. P., & Ostertag, C. (2019). Life-cycle assessment of high-strength concrete mixtures with copper slag as sand replacement. *Advances in Civil Engineering*, 6815348. https://doi.org/10.1155/2019/6815348

Hamidah, M., Azmi, I., Ruslan, M. R. A., Kartini, K., Fadhil, N. M., Shir, R. K., Newlands, M. D., & McCarthy, A. (2005). Optimisation of foamed concrete mix of different sand-cement ratio and curing conditions. In *Use of Foamed Concrete in Construction: Proceedings of the International Conference*, University of Dundee, Scotland, UK. Thomas Telford Publishing.

Hamzah, A. F., Ibrahim, M. H. W., Jamaluddin, N., Jaya, R. P., Arshad, M., Zainal Abidin, N., Manan, E., & Omar, N. (2016). Nomograph of self-compacting concrete mix design incorporating coal bottom ash as partial replacement of fine aggregates. *Journal of Engineering Applied Sciences*, *11*(7), 1671–1675.

Hou, X., Struble, L. J., & Kirkpatrick, R. J. (2004). Formation of ASR gel and the roles of C-S-H and portlandite. *Cement and Concrete Research*, *34*(9), 1683–1696. https://doi.org/10.1016/j.cemconres.2004.03.026

Kabir, S. M. A., Alengaram, U. J., Jumaat, M. Z., Yusoff, S., Sharmin, A., & Bashar, I. I. (2017). Performance evaluation and some durability characteristics of environmental friendly palm oil clinker based geopolymer concrete. *Journal of Cleaner Production*, *161*, 477–492. https://doi.org/10.1016/j.jclepro.2017.05.002

Kasemchaisiri, R., & Tangtermsirikul, S. (2008). Properties of self-compacting concrete incorporating bottom ash as a partial replacement of fine aggregate. *ScienceAsia*, *34*, 87–95. https://doi.org/10.2306/scienceasia1513-1874.2008.34.087

Kassem, M., Soliman, A., & El Naggar, H. (2018). Sustainable approach for recycling treated oil sand waste in concrete: Engineering properties and potential applications. *Journal of Cleaner Production*, *204*, 50–59. https://doi.org/10.1016/j.jclepro.2018.08.349

Kim, H. K., & Lee, H. K. (2011). Use of power plant bottom ash as fine and coarse aggregates in high-strength concrete. *Construction and Building Materials*, *25*(2), 1115–1122. https://doi.org/10.1016/j.conbuildmat.2010.06.065

Kim, H. K., Jeon, J. H., & Lee, H. K. (2012). Flow, water absorption, and mechanical characteristics of normal- and high-strength mortar incorporating fine bottom ash aggregates. *Construction and Building Materials*, *26*(1), 249–256. https://doi.org/10.1016/j.conbuildmat.2011.06.019

Kiran Kumar, M. S., Harish, K. S., Vinay, R. B., & Ramesh, M. (2018). Experimental study on partial replacement of fine aggregate by bottom ash in cement concrete. *International Research Journal of Engineering and Technology* (*IRJET*), *5*(5), 1505–1508.

Kou, S.-C., & Poon, C.-S. (2009). Properties of concrete prepared with crushed fine stone, furnace bottom ash and fine recycled aggregate as fine aggregates. *Construction and Building Materials*, *23*(8), 2877–2886. https://doi.org/10.1016/j.conbuildmat.2009.02.009

Kozłowski, M., & Kadela, M. (2018). Mechanical characterization of lightweight foamed concrete. *Advances in Materials Science and Engineering*, 6801258. https://doi.org/10.1155/2018/6801258

Kumar, D., Gupta, A., & Ram, S. (2014). Uses of bottom ash in the replacement of fine aggregate for making concrete. *International Journal of Current Engineering and Technology*, *4*(6), 3891–3895.

Kurama, H., & Kaya, M. (2008). Usage of coal combustion bottom ash in concrete mixture. *Construction and Building Materials*, *22*(9), 1922–1928. https://doi.org/10.1016/j.conbuildmat.2007.07.008

Kurama, H., Topçu, İ. B., & Karakurt, C. (2009). Properties of the autoclaved aerated concrete produced from coal bottom ash. *Journal of Materials Processing Technology*, *209*(2), 767–773. https://doi.org/10.1016/j.jmatprotec.2008.02.044

Lee, H. K., Kim, H. K., & Hwang, E. A. (2010). Utilization of power plant bottom ash as aggregates in fiber-reinforced cellular concrete. *Waste Management*, *30*(2), 274–284. https://doi.org/10.1016/j.wasman.2009.09.043

Li, X., Liu, Z., Lv, Y., Cai, L., Jiang, D., Jiang, W., & Jian, S. (2018). Utilization of municipal solid waste incineration bottom ash in autoclaved aerated concrete. *Construction and Building Materials*, *178*, 175–182. https://doi.org/10.1016/j.conbuildmat.2018.05.147

Lim, S. K., Tan, C. S., Chen, K. P., Lee, M. L., & Lee, W. P. (2013). Effect of different sand grading on strength properties of cement grout. *Construction and Building Materials*, *38*, 348–355. https://doi.org/10.1016/j.conbuildmat.2012.08.030

Madhkhan, M., & Katirai, R. (2019). Effect of pozzolanic materials on mechanical properties and aging of glass fiber reinforced concrete. *Construction and Building Materials*, *225*, 146–158. https://doi.org/10.1016/j.conbuildmat.2019.07.128

Majhi, R., & Nayak, A. N. (2019). Properties of concrete incorporating coal fly ash and coal bottom ash. *Journal of The Institution of Engineers* (*India*), *100*(3), 459–469. https://doi.org/10.1007/s40030-019-00374-y

Majhi, R., Patel, S. K., & Nayak, A. (2021a). Sustainable structural lightweight concrete utilizing high-volume fly ash cenosphere. *Advances in Concrete Construction*, *12*, 257–270. https://doi.org/10.12989/acc.2021.12.3.257

Majhi, R. K., Padhy, A., & Nayak, A. N. (2021b). Performance of structural lightweight concrete produced by utilizing high volume of fly ash cenosphere and sintered fly ash aggregate with silica fume. *Cleaner Engineering and Technology*, *3*, 100121. https://doi.org/10.1016/j.clet.2021.100121

Malaysia Energy Commission. (2017). *Malaysia energy statistics handbook*.

Mamat, R., Sani, M., & Sudhakar, K. (2019). Renewable energy in Southeast Asia: Policies and recommendations. *Science of the Total Environment*, *670*, 1095–1102.

Mangi, S. A., Ibrahim, M. W., Jamaluddin, N., Arshad M., & Ramadhansyah, P. (2019). Effects of ground coal bottom ash on the properties of concrete. *Journal of Engineering Science Technology*, *14*(1), 338–350.

Muthusamy, K., Hafizuddin, R. M., Yahaya, F. M., Sulaiman, M., Mohsin, S. S., Tukimat, N., Omar R., & Chin, S. (2018). Compressive strength performance of OPS lightweight aggregate concrete containing coal bottom ash as partial fine aggregate replacement. *IOP Conference Series*, *342*, 012099. https://doi.org/10.1088/1757-899X/342/1/012099

Muthusamy, K., Rasid, M. H., Jokhio, G. A., Budiea, A. M. A., Hussin, M. W., & Mirza, J. (2020). Coal bottom ash as sand replacement in concrete: A review. *Construction and Building Materials*, *236*, 117507. https://doi.org/10.1016/j.conbuildmat.2019.117507

Muthusamy, K., M. Rasid, M. H., Isa, N. N., Hamdan, N. H., Jamil, N. A. S., Budea, A. M. A., & Ahmad, S. W. (2021). Mechanical properties and acid resistance of oil palm shell lightweight aggregate concrete containing coal bottom ash. *Materials Today: Proceedings*, *41*(1), 47–50. https://doi.org/10.1016/j.matpr.2020.10.1001

Nambiar, E. K. K., & Ramamurthy, K. (2007). Sorption characteristics of foam concrete. *Cement and Concrete Research*, *37*(9), 1341–1347. https://doi.org/10.1016/j.cemconres.2007.05.010

Neville, A. M., & Brooks, J. J. (2010). *Concrete technology*. Prentice Hall.

Onprom, P., Chaimoon, K., & Cheerarot, R. (2015). Influence of bottom ash replacements as fine aggregate on the property of cellular concrete with various foam contents. *Journal of Advances in Materials Science Engineering*, 381704. https://doi.org/10.1155/2015/381704

Opoku, A. (2019). Biodiversity and the built environment: Implications for the Sustainable Development Goals (SDGs). *Resources*, *Conservation and Recycling*, *141*, 1–7. https://doi.org/10.1016/j.resconrec.2018.10.011

Opon, J., & Henry, M. (2019). An indicator framework for quantifying the sustainability of concrete materials from the perspectives of global sustainable development. *Journal of Cleaner Production*, *218*, 718–737. https://doi.org/10.1016/j.jclepro.2019.01.220

Patel, S., Satpathy, H., Nayak, A., & Mohanty, C. (2019). Utilization of fly ash cenosphere for production of sustainable lightweight concrete. *Journal of The Institution of Engineers* (*India*): *Series A*, *101*, 179–194. https://doi.org/10.1007/s40030-019-00415-6

Patel, S. K., & Nayak, A. N. (2021). Study on specific compressive strength of concrete with fly ash cenosphere. In B. Das, S. Barbhuiya, R. Gupta, & P. Saha (Eds.), *Lecture notes in civil engineering: Vol. 75. Recent developments in sustainable infrastructure*. Springer, Singapore. https://doi.org/10.1007/978-981-15-4577-1_47

Rafieizonooz, M., Mirza, J., Salim, M., Hussin, R. M. W., & Khankhaje, E. (2016). Investigation of coal bottom ash and fly ash in concrete as replacement for sand and cement. *Construction and Building Materials*, *116*, 15–24. https://doi.org/10.1016/j.conbuildmat.2016.04.080

Rathnayake, M., Julnipitawong, P., Tangtermsirikul, S., & Toochinda, P. (2018). Utilization of coal fly ash and bottom ash as solid sorbents for sulfur dioxide reduction from coal fired power plant: Life cycle assessment and applications. *Journal of Cleaner Production*, *202*, 934–945. https://doi.org/10.1016/j.jclepro.2018.08.204

Sachdeva, A., & Khurana, G. (2015). Strength evaluation of cement concrete using bottom ash as a partial replacement of fine aggregates. *International Journal of Science*, *Engineering and Technology*, *3*(6), 189–194.

Sani, M. S. H. M., Muftah, F., & Muda, Z. (2010). The properties of special concrete using washed bottom ash (WBA) as partial sand replacement. *International Journal of Sustainable Construction Engineering and Technology*, *1*(2), 65–76.

Sathiparan, N., & De Zoysa, H. T. S. M. (2018). The effects of using agricultural waste as partial substitute for sand in cement blocks. *Journal of Building Engineering*, *19*, 216–227. https://doi.org/10.1016/j.jobe.2018.04.023

Satpathy, H. P., Patel, S. K., & Nayak, A. N. (2019). Development of sustainable lightweight concrete using fly ash cenosphere and sintered fly ash aggregate. *Construction and Building Materials*, *202*, 636–655. https://doi.org/10.1016/j.conbuildmat.2019.01.034

Shahbaz, M., Yusup, S., Pratama, A., Inayat, A., Patrick, D. O., & Ammar, M. (2016). Parametric study and optimization of methane production in biomass gasification in the presence of coal bottom ash. *Procedia Engineering*, *148*, 409–416. https://doi.org/10.1016/j.proeng.2016.06.432

Siddique, R. (2013). Compressive strength, water absorption, sorptivity, abrasion resistance and permeability of self-compacting concrete containing coal bottom ash. *Construction and Building Materials*, *47*, 1444–1450. https://doi.org/10.1016/j.conbuildmat.2013.06.081

Siddique, R., & Cachim, P. (2018). *Waste and supplementary cementitious materials in concrete: Characterisation, properties and applications*. Woodhead Publishing.

Singh, M., & Siddique, R. (2014). Strength properties and microstructural properties of concrete containing coal bottom ash as partial replacement of fine aggregate. *Construction and Building Materials*, *50*, 246–256. https://doi.org/10.1016/j.conbuildmat.2013.09.026

Singh, M., & Siddique, R. (2015). Properties of concrete containing high volumes of coal bottom ash as fine aggregate. *Journal of Cleaner Production*, *91*, 269–278. https://doi.org/10.1016/j.jclepro.2014.12.026

Singh, M., & Siddique, R. (2016). Effect of coal bottom ash as partial replacement of sand on workability and strength properties of concrete. *Journal of Cleaner Production*, *112*, 620–630. https://doi.org/10.1016/j.jclepro.2015.08.001

Singh, N., Mithulraj, M., & Arya, S. (2018). Influence of coal bottom ash as fine aggregates replacement on various properties of concretes: A review. *Resources, Conservation and Recycling*, *138*, 257–271. https://doi.org/10.1016/j.resconrec.2018.07.025

Tian, Y., Zhou, X., Yang, Y., & Nie, L. (2020). Experimental analysis of air-steam gasification of biomass with coal-bottom ash. *Journal of the Energy Institute*, *93*(1), 25–30. https://doi.org/10.1016/j.joei.2019.04.012

Topçu, I. B., & Bilir, T. (2010). Effect of bottom ash as fine aggregate on shrinkage cracking of mortars. *ACI Materials Journal*, *107*(1), 48–56. https://doi.org/10.14359/51663465

Yang, K.-H., Hwang, Y.-H., Lee, Y., & Mun, J.-H. (2019). Feasibility test and evaluation models to develop sustainable insulation concrete using foam and bottom ash aggregates. *Construction and Building Materials*, *225*, 620–632. https://doi.org/10.1016/j.conbuildmat.2019.07.130

Yang, K.-H., Mun, J.-H., & Kwon, S.-J. (2020). Unrestrained and restrained shrinkage behavior of sustainable lightweight concrete using air foam and bottom ash aggregates. *Journal of Materials in Civil Engineering*, *32*(10), 04020287. https://doi.org/10.1061/(ASCE)MT.1943-5533.0003375

Yao, Z. T., Ji, X. S., Sarker, P. K., Tang, J. H., Ge, L. Q., Xia, M. S., & Xi, Y. Q. (2015). A comprehensive review on the applications of coal fly ash. *Earth-Science Reviews*, *141*, 105–121. https://doi.org/10.1016/j.earscirev.2014.11.016

Yüksel, I., & Genç, A. (2007). Properties of concrete containing nonground ash and slag as fine aggregate. *ACI Materials Journal*, *104*(4), 397–403. https://doi.org/10.14359/18829

Yüksel, İ., Siddique, R., & Özkan, Ö. (2011). Influence of high temperature on the properties of concretes made with industrial by-products as fine aggregate replacement. *Construction and Building Materials*, *25*(2), 967–972. https://doi.org/10.1016/j.conbuildmat.2010.06.085

Zhang, M.-H., & Gjørv, O. E. (1990). Microstructure of the interfacial zone between lightweight aggregate and cement paste. *Cement and Concrete Research*, *20*(4), 610–618. https://doi.org/10.1016/0008-8846(90)90103-5

Zhang, M.-H., & Gjørv, O. E. (1992). Penetration of cement paste into lightweight aggregate. *Cement and Concrete Research*, *22*(1), 47–55. https://doi.org/10.1016/0008-8846(92)90135-I